FABRICATION OF POLY(ETHYLENE OXIDE) AND CELLULOSE NANOCRYSTAL/ POLY(ETHYLENE OXIDE) FIBERS BY ELECTROSPINNING

Đến tòa soạn ngày 09/03/2021

Doan Van Hong Thien, Ho Diep Long, Dan-Thuy Van-Pham
Department of Chemical Engineering, Can Tho University
Chanh-Nghiem Nguyen
Department of Automation Technology, Can Tho University

TÓM TẮT

CHẾ TẠO SỢI POLY(ETHYLENE OXIDE), SỢI (ETHYLENE OXIDE) KẾT HỢP NANOCELLULOSE BẰNG KỸ THUẬT ELECTROSPINNING

Với sự tăng trưởng nhanh chóng của nhận thức về môi trường và nhu cầu cao về việc thay thế các vật liệu không tái tạo, nghiên cứu về phát triển các vật liệu bền vững và thân thiện với môi trường đã và đang thu hút sự quan tâm của các nhà khoa học. Trong đó, nanocellulose và các vật liệu composite được gia cường bằng nanocellulose đã thu hút sự quan tâm do các đặc tính độc đáo như khả năng tái tạo, khả năng phân hủy sinh học, tính tương thích sinh học, không độc hại và thân thiện với môi trường. Trong nghiên cứu này, tinh thể nanocellulose (CNC) được phân lập từ giấy văn phòng đã qua sử dụng và được pha trộn với poly (ethylene oxide) (PEO) để chế tạo sợi nanocomposite bằng kỹ thuật electrospinning. Bên cạnh đó, sợi PEO cũng được chế tạo thành công và là cơ sở để so sánh, đánh giá sợi nanocomposite. Ảnh hưởng của các điều kiện như thành phần dung dịch, điện áp và khoảng cách giữa đầu phun và bộ thu trên hình thái của sợi điện cực đã được lần lượt khảo sát. Kết quả thực nghiệm cho thấy sợi PEO thu được có đường kính trung bình là 151 ± 25 nm và sợi CNC / PEO có đường kính trung bình là 142 ± 30 nm.

Từ khóa: *kỹ thuật electrospinning, nanocellulose, poly(ethylene oxide), sợi nano.*

1. INTRODUCTION

Rising environmental awareness all over the world has resulted in an interest in environmentally friendly materials. Biodegradable polymers have been known as promising materials. Among them, cellulose nanocrystal (CNC) and nanocellulose-based composites have attracted enormous interest owing to the unique features of CNC such as high mechanical properties, renewability, low weight, thermal stability, nanoscale dimension of CNC, and its capacity to enhance the ionic conductivity of the polymer.

CNC has been utilized to reinforce polymer matrix by solution casting [1] and electrospinning [2]. N. D. Wanasekara et al. successfully fabricated CNC/PS fibers and CNC/PVA fibers, with an average diameter of about 3 μm and 0.3 μm, respectively [2]. It was shown that CNC was locally oriented in the cross-section and a few CNC oriented along the fiber axis.

CNC/PEO composites have been studied in several fields as solid-state electrolyte [3], thermal energy storage [4], biomedical applications [5]. Chengjun et al. have found that increased amounts reduced the diameter of PEO/CNC fibers. The smallest diameter was 149 ± 49 nm [6]. It was found that CNC effectively

improved the mechanical properties of the nanofibrous mats.

CNC has been known to have different forms and properties depending upon the source material and the extraction method [1]. In this study, CNC was isolated from used office papers by means of acid hydrolysis. For CNC/PEO fiber fabrication process, CNC was added to PEO aqueous solution to produce CNC/PEO fibers by electrospinning. In this process, several parameters were investigated, namely PEO concentration, CNC:PEO ratio, the applied voltage, and the distance between the tip and the collector on the morphology of electrospun CNC/PEO fibers. Heretofore PEO fiber formation process was observed for comparison.

2. MATERIALS AND METHODS

2.1. Materials

Used office papers containing inks were collected in Can Tho City, Vietnam, for CNC production. Sodium hydroxide (96%), sodium hypochlorite (8.4%), sulfuric acid (99.9%), and acetic acid (99.95%), and poly(ethylene oxide) (PEO) (87-89%) with an average molecular weight of 400 kDa were purchased from Xilong Scientific Co., Ltd., China. Chitosan (75-85%) was provided by Sigma-Aldrich. All chemicals were used without any further purification.

2.2. Methods

2.2.1 Preparation of CNC from used office papers

CNC was isolated from used office papers utilizing alkali and bleaching treatments followed by acid hydrolysis. This procedure closely followed the preparation flow that has been successfully conducted and reported in [7,8]. Used office papers were cut into strips using a shredder (Aurora, AS1219CE, Singapore) and then cut into pieces of 0.5 × 0.5 cm. These small pieces were pulverized and alkali-treated by using 2 wt% of NaOH solution at 100 ℃ in 4 h under continuous stirring with the speed of 700 rpm, then rinsed with water until pH = 7. The dried obtained sample was bleached by using 2 wt% of NaClO solution with the addition of acetic acid solution at 70 ℃ in 1 h under continuous stirring with the speed of 700 rpm. Then the sample was rinsed with water until pH = 7 and dried.

After removing lignin, hemicellulose residuals, and any other extracts, the obtained cellulose was treated by using acid hydrolysis. 64 wt% H_2SO_4 was added dropwise into previously extracted cellulose under continuous stirring with the speed of 100 rpm and heating at 45 ℃. The reaction was terminated by adding 1 L of distilled water and rinsed with water.

2.2.2. Crystallinity index and the average crystalline dimension of CNC

In this study, CNC was isolated following the previously reported preparation flow [7,8]. However, the source material was used office papers which were different from the used newspaper. The crystallinity index (*Cr.I*) and the average crystallinine dimension (*D*) were calculated from the XRD data obtained by the D2 PHASER X-ray diffractometer (Bruker, Germany). The *Cr.I* was determined by using Segal's method by the following equation.

$$Cr.I(\%) = \frac{I_{002} - I_{am}}{I_{002}} \times 100 \quad (1)$$

where I_{002} and I_{am} are the intensity area of the peak at 2θ = 21.7° and the intensity area of the amorphous scatter at 2θ =11.8°, respectively.

The mean size of crystallite (D) was estimated using the Debye-Scherer equation [9]

$$D = \frac{k\lambda}{\beta_{1/2}\cos\theta} \quad (2)$$

where k is Scherer constant (0.91), λ is the wavelength of the radiation (λ=0.15406 nm), $\beta_{1/2}$ is the full width at the half maximum (FWHM) of the XRD peak, and 2 θ is the scattering angle of the peak at 21.7°.

2.2.3. Preparation of PEO fibers

In this study, PEO aqueous solution with various concentrations (60, 70, 80, 90, 100,

110 mg/mL) was prepared by continuous stirring at 90 °C in 1 h and stabilized in 24 h. The solution was placed in a syringe of 1 mL with a 0.4 mm stainless steel needle for electrospinning. The needle was connected to a high voltage power supply to generate positive DC voltage from 8 – 18 kV. The flow rate of the solution was fixed at 0.6 mL/h. A rotating collector covered by a piece of aluminum foil was placed under the capillary needle tip. The distance between the tip and the collector was investigated from 10 to 16cm.

2.2.4. Preparation of CNC/PEO fibers

CNC with a CNC/PEO ratio of 1:9; 2:8, and 3:7 was added to PEO aqueous solution. In this study, besides factors of PEO concentration, the CNC:PEO ratio, the applied voltage, and the distance between the tip and the collector, was investigated as well.

2.2.5. Characterization of fiber

The morphology of electrospun fibers was first observed using an optical microscope (Nikon, ECLIPSE LV100POL, Japan). The optimal PEO and CNC/PEO fibers were then confirmed by using a Scanning Electron Microscope (SEM) (Jeol/JSM-6480LV Japan). GNU Image Manipulation Program was applied to determine the average diameter and the distribution of electrospun fibers. The Fourier transform infrared spectrometer (Perkin Elmer, UK) was utilized for analyzing the CNC, PEO fibers, and CNC/PEO fibers.

3. RESULTS AND DISCUSSION

3.1. XRD analysis of CNC

Figure 1 shows the XRD diffraction pattern to calculate the crystallinity index and the average crystalline dimension of the CNC product. Diffraction peaks at 2θ = 11.8, 20, and 21.7° were close to the typical peaks of cellulose crystal structures as previously reported elsewhere [7, 10]. Using Equations 1 and 2, the Crystallinity index (*Cr.I*) and average crystalline dimension (D) of CNC were 78% and 5.65 nm, respectively.

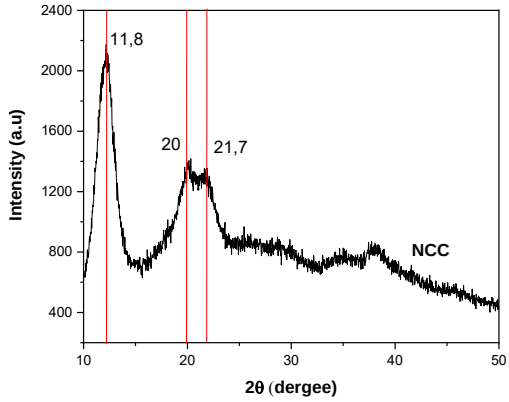

Figure 1. XRD patterns of the extracted CNC

3.2. Observation of PEO fibers morphology

Within the experiments for the study of PEO concentration, the applied voltage and distance between the tip and the collector were 12 kV and 12 cm, respectively. The morphology of electrospun PEO was significantly affected by PEO concentration captured by an optical microscope (Fig. 2). The increase in PEO concentration promoted the viscosity of the solution, leading to enhancement in the entanglement force between polymer chains of PEO [11].

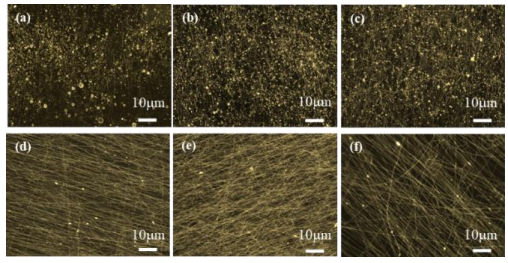

Figure 2. Morphology of electrospun PEO obtained under various PEO concentration (a) 60; (b) 70; (c) 80; (d) 90; (e) 100 and (f) 110 mg/mL

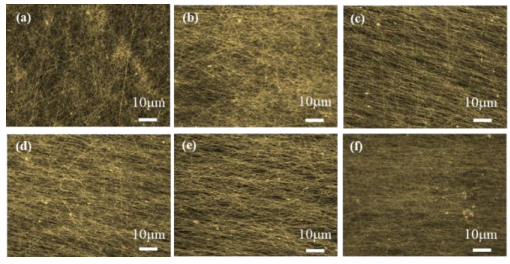

Figure 3. Morphology of electrospun PEO obtained under various applied voltage (a) 8; (b) 10; (c) 12; (d) 14; (e) 16 and (f) 18 kV

Therefore, as PEO concentration was lower than 90 mg/mL, PEO the bead-in-string morphology was obtained instead of PEO fibers. When PEO concentration was from 90 to 110 mg/mL, PEO fibers were detected. The continuously straightest PEO fibers were formed as PEO concentration was 100 mg/mL. Therefore, the PEO concentration and the distance between the tip and the collector were 100 mg/mL and 12 cm, respectively, to study the applied voltage. When the electrical field with low voltage was used, the produced fibers were not well oriented, as shown in Fig. 3a and Fig. 3b. The stronger electrical force induced by higher voltage caused the repulsive force between charges leading to fiber formation (Fig. 3c). However, as the applied voltage was too high, the fiber diameter increased (Fig. 3d, e). While the fixed flow rate controlled rate that solution spread out of the needle was at 0.6 mL/h, there would not be enough time for the electrospun jet to decrease its diameter via solvent evaporation in case of high applied voltage [12]. As the applied voltage increased to 18kV, more tangled fibers were obtained. The suitable applied voltage was 12 kV.

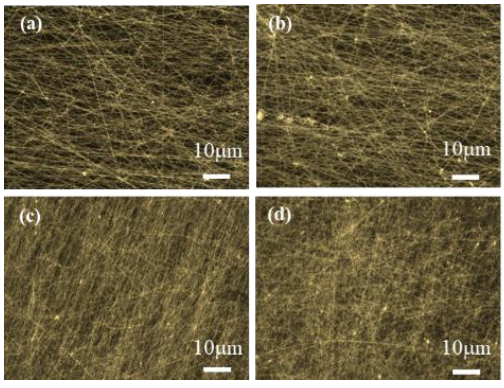

Figure 4. Morphology of electrospun PEO obtained under various distance between the tip and the collector (a) 10; (b) 12; (c) 14; (d) 16 cm.

It was shown that as the distance between the tip and the collector increased, the fiber diameter decreased (Fig. 4a, 4b). Simultaneously, the fiber disorder was formed (Figure 4c, 4d). Therefore, the optimal distance was 10cm.

3.3. Observation of CNC/PEO fibers morphology

The morphology of electrospun CNC/PEO was affected by PEO concentration as the CNC:PEO ratio, the applied voltage, and the distance between the tip and the collector were 2:8; 14 kV and 15cm (Fig. 5). It was found that at lower PEO concentration (60 mg/mL), the bead-in-string morphology existed. As the PEO concentration increased from 70 to 90 mg/mL, the CNC/PEO fibers were improved. This could be explained by the increase of the solution viscosity leading to the decrease in the evaporation of the solvent. The stability in the solvent evaporation speed led to an increase in the fiber formation. Therefore, the diameter of fibers was increased. However, at higher PEO concentrations (100 and 110 mg/mL), as the viscosity was too high, the polymer chains stuck inside the tip, restraining the Taylor cone's stability [13]. As a result, the optimal PEO concentration in CNC/PEO mixture was 90 mg/mL.

Different electrospun CNC/PEO morphology was obtained under various CNC:PEO ratios as PEO concentration, the applied voltage, and the distance between the tip and the collector were 90 mg/mL, 14 kV, and 15cm (Fig. 6). Beads within single fibers were rarely visible in the electrospun CNC/PEO (1/9). As the CNC content increased, the bead-in-string was detected instead of straight fibers in the case of CNC:PEO (2:8 and 3:7). This could be explained by the decrease in the viscosity of the solution as CNC was blended in the mixture. It was reported that the viscosity of PEO/CNC suspensions decreased significantly after CNC was added to PEO solution because CNC disrupted the PEO chain – chain interactions and entanglements [6]. As a consequence, the entanglement force was reduced and decelerated the fiber formation.

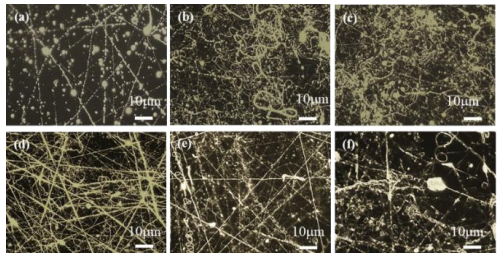

Figure 5. Morphology of electrospun CNC/PEO obtained under various PEO concentration (a) 60; (b) 70; (c) 80; (d) 90; (e) 100 and (f) 110 mg/mL

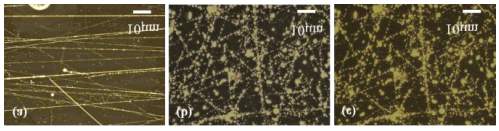

Figure 6. Morphology of electrospun CNC/PEO obtained under various CNC:PEO ratio (a) 1:9; (b) 2:8; (c) 3:7

The morphology of electrospun CNC/PEO was also affected by the applied voltage as PEO concentration, the CNC:PEO ratio, and the distance between the tip and the collector were 90 mg/mL, 1:9 and 15cm (Fig. 7). At low voltage (10 kV), the large beads were obtained (Fig. 7a). The stronger electrical force induced by higher voltage caused the repulsive force between charges leading to fiber formation (Fig. 7b). However, as the applied voltage was too high, the fast flow rate enhanced the entanglement of the fibers. Therefore, the suitable applied voltage was 12 kV.

As the PEO concentration, the CNC:PEO ratio, and the applied voltage between the tip and the collector were fixed at 90 mg/mL; 1:9 and 12 kV, the entangle fibers were formed in case of the shortest distance (Fig.). As the distance was 12 cm, the uniform straight fibers were obtained. However, as the distance kept increasing, the bead-in-string morphology was detected. Therefore, the optimal distance in this study was 12 cm.

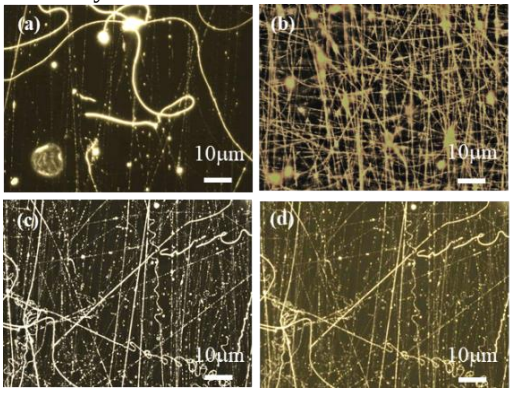

Figure 7. Morphology of electrospun CNC/PEO obtained under various applied voltage (a) 10; (b) 12; (c) 14; (d) 16 kV

3.4. FTIR spectroscopy analysis

The FTIR spectra of the extracted NCC, PEO fibers, and CNC/PEO fibers are shown in Figure 9.

The peaks in the 3333-3500 cm^{-1} and 1640 cm^{-1} regions corresponded to the presence of O-H stretching vibration and O-H bending of the absorbed water in both CNC and PEO fibers. The overlapped CH_2 stretching in PEO and C-H stretching in CNC led to a significant increase in the absorption bands of CNC/PEO at 2891 cm^{-1}. Similarly, the gain at 1101 cm^{-1} in CNC/PEO was caused by the overlapped absorption of C-OH deformation in CNC and C-O-C stretching vibration in PEO. The absorption intensity at 1468 cm^{-1} in CNC/PEO increased due to the CH_2 bending presented in both CNC and PEO [13].

3.5. Morphology and diameter of the optimum PEO and CNC/PEO fibers

Figure 10 shows the SEM images of the optimum PEO and CNC/PEO fibers. The uniform nanofibers were obtained for both the optimum PEO and CNC/PEO fibers. The average diameter of the optimum PEO fibers was about 151 ± 25 nm. As CNC was blended in PEO mixture, the average diameter of the optimum CNC/PEO fibers slightly reduced to 142 ± 30 nm, which was smaller than earlier reported [6]. The reduction in the average diameter might result from the decrease in the viscosity of the mixture due to CNC content.

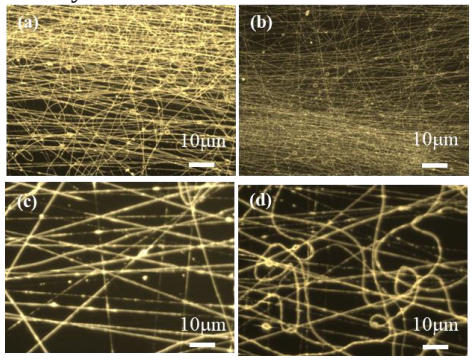

Figure 8. Morphology of electrospun CNC/PEO obtained under various distance between the tip and the collector (a) 10; (b) 12; (c) 14; (d) 16 cm

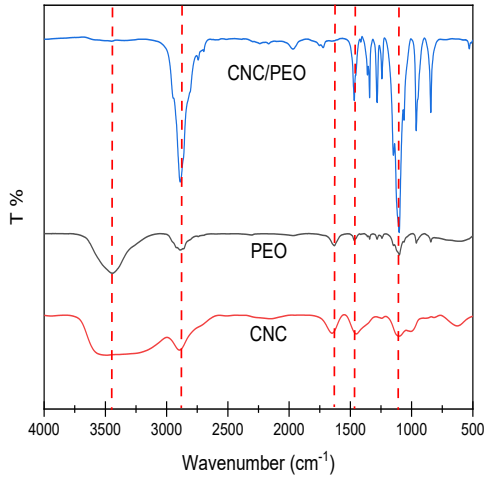

Figure 9. FTIR spectra of CNC, PEO, CNC/PEO

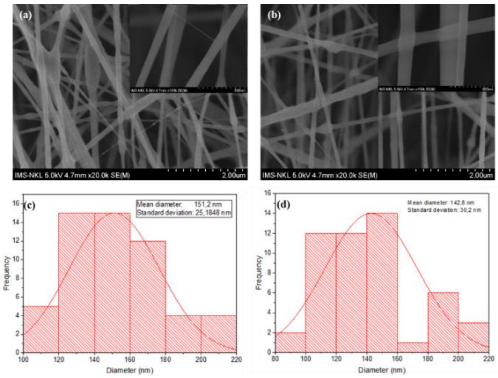

Figure 10. SEM images and diameter of (a) PEO fibers and (b, d) CNC/PEO fibers

4. CONCLUSIONS

In this study, CNC with the crystallinity index of 78% and the average crystalline dimension of 5.65 nm was extracted from used office paper. The uniform PEO and CNC/PEO fibers were successfully produced by using electrospinning. The almost homogenous electrospun fibers from PEO solution and CNC/PEO suspension were successfully fabricated. Suitable electrospinning parameters for 100 mg/mL PEO solution included a 12 kV voltage with a needle tip to the collector of 10 cm. For CNC/PEO suspension with the ratio of 1:9, the suitable voltage and distance between the tip and the collector were 12 kV and 12 cm, respectively. With the addition of CNC in PEO solutions, the fiber diameter was decreased from 151 ± 25 nm to 142 ± 30 nm.

Acknowledgments

This study is funded in part by the Can Tho University Improvement Project VN14-P6, supported by a Japanese ODA loan.

REFERENCES

1. Thakur, M.K., V.K. Thakur, and R. Prasanth, *Nanocellulose-Based Polymer Nanocomposites: An Introduction*, in *Nanocellulose Polymer Nanocomposites*. 2014. p. 1-15.

2. Wanasekara, N.D., R.P.O. Santos, C. Douch, E. Frollini, and S.J. Eichhorn (2015). *Orientation of cellulose nanocrystals in electrospun polymer fibres.* Journal of Materials Science, 51(1): p. 218-227.

3. Qin, H., K. Fu, Y. Zhang, Y. Ye, M. Song, Y. Kuang, S.-H. Jang, F. Jiang, and L. Cui (2020). *Flexible nanocellulose enhanced Li+ conducting membrane for solid polymer electrolyte.* Energy Storage Materials, 28: p. 293-299.

4. Shi, Z., H. Xu, Q. Yang, C. Xiong, M. Zhao, K. Kobayashi, T. Saito, and A. Isogai (2019). *Carboxylated nanocellulose/poly(ethylene oxide) composite films as solid–solid phase-change materials for thermal energy storage.* Carbohydrate Polymers, 225: p. 115215.

5. Lu, Y., H.L. Tekinalp, C.C. Eberle, W. Peter, A.K. Naskar, and S. Ozcan (2014). *Nanocellulose in polymer composites and biomedical applications.* Tappi J, 13(6): p. 47-54.

6. Zhou, C., R. Chu, R. Wu, and Q. Wu (2011). *Electrospun polyethylene oxide/cellulose nanocrystal composite nanofibrous mats with homogeneous and heterogeneous microstructures.* Biomacromolecules, 12(7): p. 2617-25.

7. Van-Pham, D.-T., T.Y.N. Pham, M.C. Tran, C.-N. Nguyen, and Q. Tran-Cong-Miyata (2020). *Extraction of thermally stable cellulose nanocrystals in short processing time from waste newspaper by conventional acid hydrolysis.* Materials Research Express, 7(6): p. 065004.

8. Nang An, V., H.T. Chi Nhan, T.D. Tap, T.T.T. Van, P. Van Viet, and L. Van Hieu (2020). *Extraction of High Crystalline Nanocellulose from Biorenewable Sources of Vietnamese Agricultural Wastes.* Journal of Polymers and the Environment, 28(5): p. 1465-1474.

9. Campano, C., R. Miranda, N. Merayo, C. Negro, and A. Blanco (2017). *Direct production of cellulose nanocrystals from old newspapers and recycled newsprint.* Carbohydr Polym, 173: p. 489-496.

10. Van-Pham, D.-T., T. Thi Bich Quyen, P. Van Toan, C.-N. Nguyen, M.H. Ho, and D. Van Hong Thien (2020). *Temperature effects on electrospun chitosan nanofibers.* Green Processing and Synthesis, 9(1): p. 488-495.

11. Cramariuc, B., R. Cramariuc, R. Scarlet, L.R. Manea, I.G. Lupu, and O. Cramariuc (2013). *Fiber diameter in electrospinning process.* Journal of Electrostatics, 71(3): p. 189-198.

12. Li, D. and Y. Xia (2004). *Electrospinning of Nanofibers: Reinventing the Wheel?* Advanced Materials, 16(14): p. 1151-1170.

13. McKiernan, R.L., A.M. Heintz, S.L. Hsu, E.D.T. Atkins, J. Penelle, and S.P. Gido (2002). *Influence of Hydrogen Bonding on the Crystallization Behavior of Semicrystalline Polyurethanes.* Macromolecules, 35(18): p. 6970-6974.